

# Robust Feature Extraction and Classification of EEG Spectra for Real-time Classification of Cognitive State

<p><i>John Wallerius</i> <i>Leonard J. Trejo</i> Pacific Development and Technology, LLC Mountain View, CA jwallerius@pacdel.com</p>	<p><i>Robert Matthews</i> Quantum Applied Science and Research San Diego, CA robm@quasarusa.com</p>
<p><i>Roman Rosipal</i> Austrian Research Institute For Artificial Intelligence Vienna, Austria roman@oefai.at</p>	<p><i>John A. Caldwell</i> Brooks Air Force Base San Antonio, TX John.Caldwell@brooks.af.mil</p>

## Abstract

We developed an algorithm to extract and combine EEG spectral features, which effectively classifies cognitive states and is robust in the presence of sensor noise. The algorithm uses a partial-least squares (PLS) algorithm to decompose multi-sensor EEG spectra into a small set of components. These components are chosen such that they are linearly orthogonal to each other and maximize the covariance between the EEG input variables and discrete output variables, such as different cognitive states. A second stage of the algorithm uses robust cross-validation methods to select the optimal number of components for classification. The algorithm can process practically unlimited input channels and spectral resolutions. No a priori information about the spatial or spectral distributions of the sources is required. A final stage of the algorithm uses robust cross-validation methods to reduce the set of electrodes to the minimum set that does not sacrifice classification accuracy. We tested the algorithm with simulated EEG data in which mental fatigue was represented by increases frontal theta and occipital alpha band power. We synthesized EEG from bilateral pairs of frontal theta sources and occipital alpha sources generated by second-order autoregressive processes. We then excited the sources with white noise and mixed the source signals into a 19-channel sensor array (10-20 system) with the three-sphere head model of the BESA Dipole Simulator. We generated synthetic EEG for 60 2-second long epochs. Separate EEG series represented the alert and fatigued states, between which alpha and theta amplitudes differed on average by a factor of two. We then corrupted the data with broadband white noise to yield signal-to-noise ratios (SNR) between 10 dB and -15 dB. We used half of the segments for training and cross-validation of the classifier and the other half for testing. Over this range of SNRs, classifier performance degraded smoothly, with test proportions correct (TPC) of 94%, 95%, 96%, 97%, 84%, and 53% for SNRs of 10 dB, 5 dB, 0 dB, -5 dB, -10 dB, and -15 dB, respectively. We will discuss the practical implications of this algorithm for real-time state classification and an off-line application to EEG data taken from pilots who performed cognitive and flight tests over a 37-hour period of extended wakefulness.

## 1 Introduction

Laboratory and operational research have shown that real-time classification of cognitive states, such as mental fatigue, may be performed using physiological measures, such as EEG recordings, as predictors or correlates of those states (St. John, Kobus & Morrison, 2003). The purpose of this study was to code and test an algorithm for real-time classification of fatigue states, identify subsets of EEG electrodes that provide adequate performance in predicting cognitive state, and quantify the effect of reduced signal-to-noise ratio (SNR) on the accuracy of the method. We sought to address five specific objectives: a) design an EEG-based computational system for classification of cognitive states, b) simulate and test the effects of reduced electrode density on the accuracy of classification, c) simulate and test the effects of reduced signal-to-noise ratio (SNR) on the accuracy of classification, d) test the effects of reduced electrode density and SNR in human EEGs from a fatigue-inducing task, e) estimate the range of useful electrode densities and SNRs for robust EEG-based classification of fatigue states.

## 2 Design of the EEG-based classifier

### 2.1 Selection of EEG features

Previous studies have reported changes in the EEG spectrum as alertness declines. For example, the proportion of low frequency EEG waves, such as theta and alpha rhythms, may increase while higher frequency waves, such as beta rhythms may decrease. In one study, as alertness fell and error rates rose in a vigilance task, researchers found

progressive increases in EEG power at frequencies centered near 4 and 14 Hz (Makeig and Inlow, 1993). Thus, the relative power of theta, alpha, and other EEG rhythms may serve to indicate the level of fatigue that subjects experience. However, the EEG spectral changes that relate to cognitive fatigue, in the absence of alertness decrements are unclear because most experiments have used vigilance-like paradigms to examine fatigue or short experimental sessions which induce high workload. The patterns of change in EEG that follow the onset of cognitive fatigue appear to be complex and subject-dependent (Gevins, et al., 1990). For these reasons, we designed our algorithm to work with high-resolution estimates of the multi-channel EEG frequency spectrum. Multi-electrode power spectra of individual EEG segments served as the EEG features for training and testing the classifier.

## 2.2 The PLS algorithm

Recently, a new algorithm derived from machine learning and statistical pattern recognition has proven to be effective for feature extraction and classification of EEG data (Rosipal & Trejo, 2001; Rosipal, Trejo, & Matthews, 2003). The method relies on a core algorithm of partial least squares (PLS). Similar to principal components regression (PCR), PLS is a method based on the projection of input (explanatory) variables to the latent variables (components). However, in contrast to PCR, PLS creates the components by modeling the relationship between input and output variables while maintaining most of the information in the input variables. PLS is useful in situations such as EEG analysis, where the number of explanatory variables exceeds the number of observations and/or a high level of multi-collinearity among those variables is assumed. The PLS method has been paired with support vector classifiers and linear classifiers for robust classification (Rosipal, et al., 2003). Combining PLS with computational kernels (KPLS) allows for extraction of a larger number of PLS components than other methods. This may be useful for isolating unique sources of variance in EEG data, much like independent components analysis (ICA, Bell and Sejnowski, 1995). Unlike ICA, KPLS methods lead to unambiguous results that lend themselves to automatic interpretation. Both linear and non-linear kernels may be applied, the latter allowing for classification of complex multivariate distributions of data. In the experiments documented in this paper, we used a linear kernel. Successful applications of this method have been documented in real-time processing of human EEG for brain-computer systems (Trejo, et al., 2003) and modeling and measuring cognitive fatigue (Trejo et al., 2004).

We regard the power spectral density of single EEG epochs of  $C$  channels and  $F$  spectral lines as a vector  $\mathbf{x}$  ( $M$ ), with  $M = C \times F$  dimensions. Each  $\mathbf{x}_i$  ( $i = 1, 2, \dots, n$ ) is a row vector of a matrix of explanatory variables,  $\mathbf{X}$  ( $n \times M$ ), with  $M$  variables and  $n$  observations. The  $n$  observations are the power spectral densities or PSDs of single EEG epochs from two classes, (e.g., experimental conditions, alert/fatigued, etc.). We regard the class membership of each EEG epoch as a matrix  $\mathbf{Y}$  ( $n \times 1$ ) in which Class 1 is assigned the value 1 and Class 2 is assigned the value -1. PLS models the relationship between the explanatory variables and class membership by decomposing  $\mathbf{X}$  and  $\mathbf{Y}$  into the form

$$\begin{aligned}\mathbf{X} &= \mathbf{TP}^T + \mathbf{F} \\ \mathbf{Y} &= \mathbf{UQ}^T + \mathbf{G}\end{aligned}$$

where the  $\mathbf{T}$  and  $\mathbf{U}$  are ( $n \times p$ ) matrices of  $p$  extracted score vectors (components or latent vectors), the ( $N \times p$ ) matrix  $\mathbf{P}$  and the ( $M \times p$ ) matrix  $\mathbf{Q}$  are matrices of loadings, and the ( $n \times N$ ) matrix  $\mathbf{F}$  and the ( $n \times M$ ) matrix  $\mathbf{G}$  are matrices of residuals. PLS seeks to maximize the covariance between the components of the explanatory variables and class membership. We use a method known as the nonlinear iterative partial least squares algorithm (NIPALS), which finds weight vectors  $\mathbf{w}$ ,  $\mathbf{c}$  such that

$$\max_{\|\mathbf{t}\| = \|\mathbf{s}\| = 1} [\text{cov}(\mathbf{X}\mathbf{r}, \mathbf{Y}\mathbf{s})]^2 = [\text{cov}(\mathbf{X}\mathbf{w}, \mathbf{Y}\mathbf{c})]^2 = [\text{cov}(\mathbf{t}, \mathbf{u})]^2$$

where  $\text{cov}(\mathbf{t}, \mathbf{u}) = \mathbf{t}^T \mathbf{u} / n$  denotes the sample covariance between the score vectors  $\mathbf{t}$  and  $\mathbf{u}$ . Application of the weight vectors to normalized data produces component scores that serve as inputs to a classifier. We have tested both discretized linear regression (DLR) and support vector classifiers (SVC), and found that in most cases, DLR produces results that are nearly equal to SVC. For this study we rely exclusively on the DLR method.

## 2.3 High-level design of the classifier

The main blocks of the classifier development procedure are data preprocessing, classifier construction, electrode reduction, and SNR reduction (Figure 1). Each block includes several components or steps, as shown in Table 1.

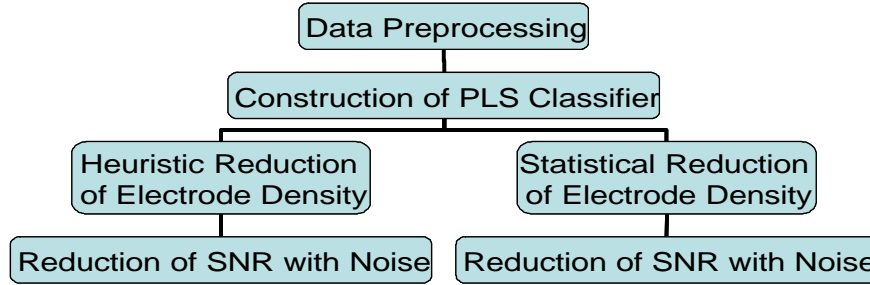


**Figure 1:** Block diagram of classifier development plan.

## 2.4 Simulation of EEG and classifier performance tests

We developed a novel system for simulation of EEG sources using autoregressive models (Anderson, Stolz, & Shamsunder, 1995; Figure 2A). This system served to create simulated EEG for testing the classifier with known inputs and SNR level. We simulated a 4-dipole EEG system as a summation of four independent autoregressive processes (BESA Dipole Simulator, MEGIS Software GmbH, Gräfelfing, Germany). The dipoles were situated symmetrically in frontal cortex and parietal cortex. The frontal pair of dipoles approximated sources of EEG theta rhythms, while the parietal pair approximated sources of alpha rhythms. We used the dipole simulator to run a forward solution through the BESA default 3-sphere head model to obtain the source-electrode coupling matrix between these dipole sources and a standard 10-20 system electrode montage (19 electrodes). Using this matrix and exciting the sources with white noise we generated pseudo EEG with properties suitable for testing the effects of noise and electrode density. Using a public-domain autoregressive model estimation package (Hayes, 1999) we solved for the best fitting AR models from the source model output (prior to spatial mixing) and verified that we could recover the model coefficients.

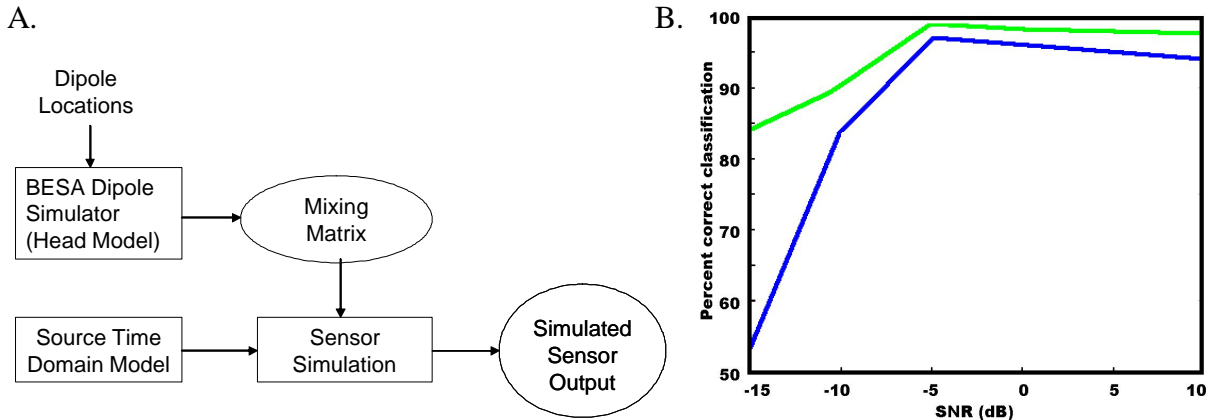


**Figure 2:** A. System for simulation of multi-channel EEG sources. B. KPLS classifier accuracies for simulated EEG data as a function of SNR. Green line is for training set, blue line is for test set.

We also estimated EEG and fatigue effects and chose reasonable parameters for mimicking the effects of cognitive fatigue (Trejo, et al., 2004) on the pseudo EEG signals. Fatigue was represented by a 50% increase in parietal alpha source amplitudes and a 25% increase in frontal theta source amplitudes over baseline conditions.

We adapted our PLS classifier code to run in Matlab (The Mathworks, Natick, MA) with visualization tools to allow us to inspect the latent variables (components) that are used to classify fatigue periods with reduced electrode density and noise effects. The generator and classifier components which had previously been tested individually are integrated in a single Matlab software system. We also made some adjustments to the code to facilitate efficiently searching the parameter space of SNRs and sensor subsets. We then determined the optimal classifier structure and parameters for the pseudo EEG signals. We performed several informal tests, which verified that our simulation: a) generates realistic EEG data for non-fatigued and fatigued states, b) derives a PLS classification model from a training subset of the simulated data, c) validates the classification model with additional simulated data.

Table 1. Procedure for development of KPLS classifiers. A. Data preprocessing. B. Construction of the PLS classifier. C. Heuristic reduction of electrode density. D. Statistical reduction of electrode density. E. SNR reduction.

A. Data Preprocessing	
1	Visual inspection of data
2	Rejection of high artifact / bad data segments
3	EOG artifact removal
4	Bandpass filtering and downsampling
5	Epoch segmentation (10-s segments)
6	Frequency spectrum estimation
7	Binary epoch categorization (normal = 1, fatigued = -1) according to time on task.
B. Construction of the PLS Classifier	
1	Partition epochs into training and test sets.
a	Randomly partition training set into equal-sized estimation and validation sets.
b	Use the estimation set to compute a linear PLS model of the binary epoch categories and record test proportion correct (TPC) for the validation set.
c	Repeat steps a. and b. for model orders (1, 2... 10 PLS components) and record TPC.
d	From the 10 PLS models of step c., choose the PLS model order that optimizes the TPC.
2	Compute final PLS model with the fixed order of step 1d and apply to the test set to obtain TPC.
C. Heuristic Reduction of Electrode Density	
1	Choose electrode regions that optimize electrode density and ease of placement.
a	Select electrodes for two density levels for each region
i	An oversampled level with 2-4 electrodes per region
ii	A critically sampled level with 1-2 electrodes per region
b	Define special sets of frontal electrodes (FP1, FPz, FP2, with and without Fz).
2	Construct a PLS classifier for each electrode set and record the TPCs for training and test sets.
D. Statistical Reduction of Electrode Density	
1	Start with the PLS model for the full set of electrodes.
a	Order the electrodes by the 75 <sup>th</sup> percentile of the weights for each PLS component.
b	For the first PLS component, select the electrode set of the model that maximizes TPC.
c	Deflate the input matrix by removing the influence of the first component.
d	Re-compute the PLS model with only the electrodes selected in b. and the deflated input matrix and select the electrode set that maximizes TPC for the second component.
e	Repeat b. – c. for up to 10 PLS components (Example: 1st component: electrodes 1 5 7 12; 2nd component: electrodes 3 2 5 4 6 7 etc.
f	Retain the electrode set that is the union of the sets for the 10 components (fully automated) or,
g	Retain the electrode set that “makes sense” after inspection of the components (supervised).
2	Choose two electrode densities based on minimizing PLS components and maximizing TPC values.
a	The oversampled set keeps TPC near the level of the full set on the curve of decreasing TPC vs. electrode density.
b	The critically sampled set keeps TPC near the 80% level on the curve of TPC vs. electrode density.
E. SNR Reduction	
1	For each electrode set, add Gaussian noise to reduce SNR in EEG segments in the test set over six levels (dB): -3, -6, -9, -12, -15, -18.
2	Add noise to the test set data for each model, without recomputing the model. Then re-compute the noise-corrupted test-set TPCs. This simulates a classifier which is fixed and is subject to operational noise contamination. Repeat this for all the models developed on noise-free data: the complete set, the heuristically reduced sets, and the statistically reduced sets.

Finally, we formally tested the effects of electrode density and noise on classification accuracy of fatigue states represented by the pseudo EEG signals (Figure 2B). The signals consisted of 60 segments of 2-s length, split into training and test sets of 30 segments each. Noise was manipulated as a factor with six discrete SNR levels ranging from +10 to -15 dB. The dependent measure was the test percentage correct (TPC) for equal-sized test sets of EEG segments from the fatigue and baseline conditions. TPC ranged from 98% to 99% for training data between SNRs of +10 and -5 dB, and then declined to 84% at -15 dB. TPC ranged from 94% to 97% for test data between SNRs of +10 and -5 dB, and then declined to 53% at -15 dB. As expected, TPC fell to chance accuracy (50%) for low SNR levels. In our experience, human EEG signals from operational settings fall in the higher range of these SNRs (above zero), suggesting that the algorithm will perform satisfactorily in the presence of recording noise.

### 3 Test classifier testing system with human EEG.

Dr. John Caldwell of Brooks Air Force Base kindly obtained official authorization to provide EEG data for two subjects from a study of the effects of fatigue over a period of 37 hours of sustained wakefulness in pilots (Caldwell, et al., 2003). This study concluded that:

“Over the past 30 years, fatigue has contributed to a number of Air Force mishaps. Resource cutbacks combined with increased operational tempos, sustained operations, and night fighting could exacerbate the problem. Extended wakefulness and circadian factors can be especially problematic in military aviation where mission demands sometimes necessitate flights as long as 17-44 hours. To effectively counter fatigue in such operations, the effects of this threat must be objectively measured and understood. This study assessed F-117A pilots during a 37-hour period of continuous wakefulness. Although none of the pilots crashed, substantial decrements were found in flight skills, reaction times, mood, and brain activation as early as after the 26<sup>th</sup> hour of continuous wakefulness. The greatest flight degradations occurred after 27-33 hours awake, even though many pilots believed their worst performance was earlier. The decrements found in this relatively-benign test environment may be more serious under operational conditions unless personnel anticipate the most dangerous times and administer valid fatigue countermeasures.”

We acquired 1.6 gigabytes of EEG and EOG data for two subjects from that study and visually assessed levels of EOG artifact and data integrity using graphical displays. We also developed a strategy for labeling the data sets for training and testing of the classifier. We also received confirmation that the data we received were from two subjects for whom there was psychometric evidence of significant fatigue over time, as indicated by the Profile of Mood States and the Visual Analog Mood Scales. We developed classifiers for these data by assuming that the chronologically earlier data represents relatively non-fatigued states, and the data near the end of the 37 hour testing period represents highly fatigued states. We selected an early test period as non-fatigued and a later test period as fatigued. Respectively, these times were 2100 on day 1 versus 1900 on day 2 for subject 212, and 0400 on day 2 versus 1900 on day 2 for subject 220.

#### 3.1 Heuristic reduction of electrode density

We performed combined testing of the signal-to-noise reduction and heuristic electrode reduction tests for the EEG data from the Brooks AFB fatigue study. Using the methods that we developed for simulated EEG data, we trained PLS classifiers for three heuristically chosen electrode set sizes: 21 (full montage), 12 and 4 (Table 2). Our heuristic was to preserve the midline electrodes, reduce electrode densities evenly and symmetrically at off-midline sites.

Table 2. Electrodes selected by heuristic method for SNR tests.

Set Size	Electrodes
21	FP1, FPz, FP2, F7, F3, Fz, F4, F8, T3, C3, Cz, C4, T4, T5, P3, Pz, P4, T6, O1, Oz, O2
12	F3, Fz, F4, C3, Cz, C4, P3, Pz, P4, O1, Oz, O2
4	Fz, Cz, Pz, Oz

The EEG segments for training and testing the classifiers were of duration 1 s, and were drawn from the early (non-fatigued) and late (fatigued) test sessions described above. From periods of 1-minute-long eyes-open, resting EEG recordings in each session, we obtained 60 contiguous epochs, of which 30 each were randomly chosen and set aside for training and testing. For subject 212, the earliest session was 2300 hrs on Day 1 and the latest session was 1900 hrs on Day 2. For subject 220, the earliest session was 0400 hrs on Day 2 and the latest session was 1900 hrs on Day 2. After training and testing the classifiers with data to which no noise was added, we added broadband white noise to the EEG in a range of SNRs from -3 to -18 dB. The classifiers were trained once for each electrode set size and tested at each noise level. This train-and-test procedure was repeated three times for each electrode set size.

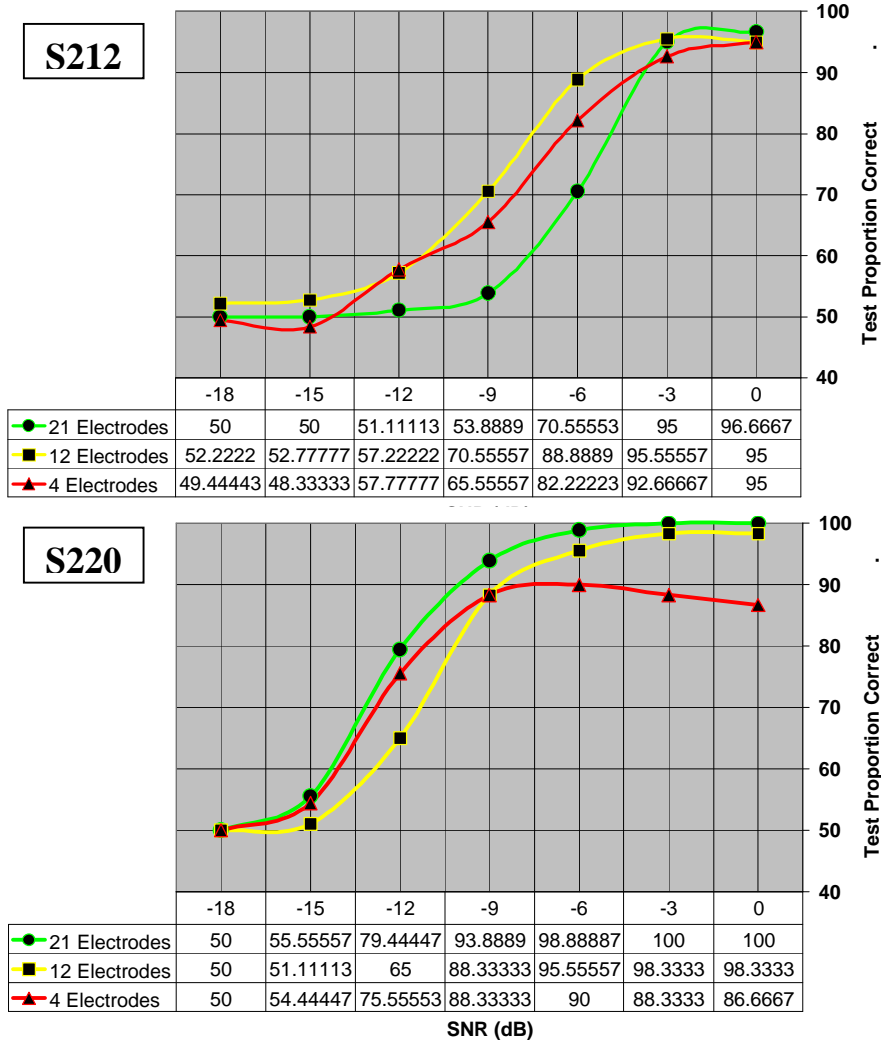


**Figure 3:** Test accuracy of KPLS classifier for non-fatigued (early) versus fatigued (late) 1-s eyes-open EEG epochs as a function of electrode set size and signal-to-noise (SNR) ratio in two subjects (S212, S220). Each point is an average of three replications of training and testing the classifier.

The method for determining the SNR was to first estimate for each epoch, the amplitude of the baseline noise recorded by the EEG amplifiers outside the EEG bandwidth. We estimated the baseline noise power,  $N$ , by calculating the average power in the highest part of the recorded EEG band, from 80 to 100 Hz in Watts/Hz. We assumed for purposes of the analysis that the noise power was approximately constant over the 0 to 100 Hz band. We used the average recorded EEG signal power in the band from 0-25 Hz as a signal estimate, which we arbitrarily set to be 0 dB SNR. We did not try to estimate the actual signal to noise ratio; we just estimated the baseline noise power and defined the recorded EEG SNR to be 0 dB. We added additional noise in 3 dB (factors of 2 in power), so that the test SNRs are as follows:  $S/N$  (no noise added)  $\implies$  0 dB,  $S/(N + aN)$  (add additional noise equal to estimated baseline noise power)  $\implies$  -3 dB, etc. The full set of SNRs tested was: 0, -3, -6, -9, -12, -15, -18 dB. As expected, classification accuracy decreased over the range of SNRs (Figure 3).

Overall, we obtained the highest accuracies with 21 electrodes, and lower accuracies with 12 and 4 electrodes, respectively. Accuracies were also higher for Subject 212 than for Subject 220. It is possible this difference derives from a larger interval between the test sessions in Subject 212 than in Subject 220. Interestingly, for Subject 220, the accuracies with 12 and 4 electrodes were both nearly 90% correct at a SNR of -9 dB, only 5% lower than for 21 electrodes. This suggests that with reasonable fatigue effects, our KPLS algorithm may be robust under conditions of severe noise contamination of the EEG, where the added noise is as large as 6 to 7 times the initial background noise

level. Since EEG recordings typically have positive SNRs, our method of estimating SNR as a multiple of background noise is conservative, because we assigned the uncorrupted recordings a SNR of 0 dB.

### 3.2 Frontal electrode sets

We also repeated the preceding tests with two special sets of three or four frontal electrodes, [FP1 FPz FP2] or [FP1 FPz FP2 Fz]. What we had in mind was to select electrodes for which application is unencumbered by scalp hair. This may be beneficial for non-contact E-field sensors and for mounting sensors in headgear. In general, the effects of limiting the set to these four frontal electrodes were positive. Surprisingly, TPCs for the frontal set were slightly higher than for the four midline electrodes, at SNR levels of about -6 dB and below, although the maximal TPCs were lower than for 21 electrodes (Figure 4). In a similar manner, addition of electrode Fz improved high-SNR TPCs but reduced low-SNR TPCs. Thus in the region of the TPC/SNR curve that covers the worst expected levels of noise degradation, the frontal sets performed as well as or better than the midline set. In the other subject (212, not shown), the TPCs for the frontal set between -6 and -9 dB ranged from 82 to 85%. Overall, the results are encouraging for an easily-applied frontal set of electrodes in fatigue classification systems.

### 3.3 Statistical reduction of electrode density

Our final analyses considered the results of a selection of reduced electrode sets by a statistical learning method. For each subject we performed the steps outlined in Table 1, using a limit of 10 PLS components in each PLS model.

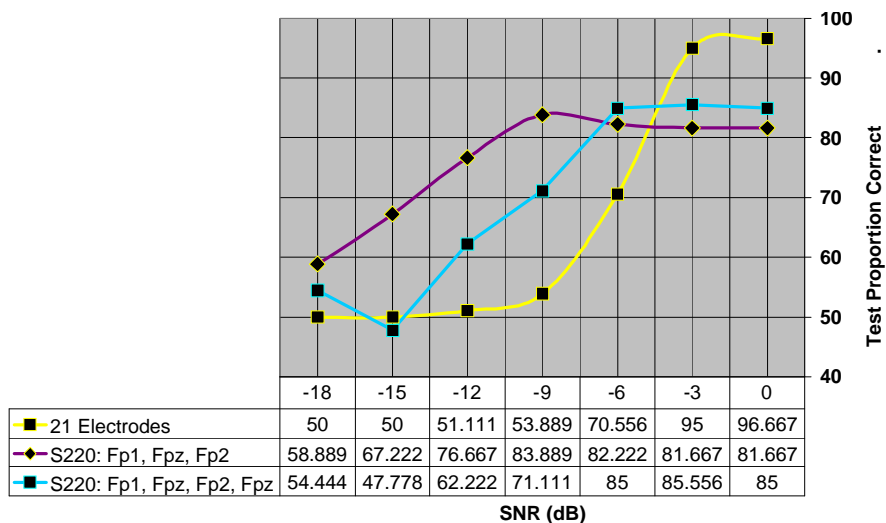


**Figure 4:** Test accuracy of PLS classifier for non-fatigued (early) versus fatigued (late) eyes-open EEG epochs as a function of electrode set size (21 or Frontal set) and signal-to-noise (SNR) ratio in subject 220. Each point is an average of three replications of training the classifier.

Each model was based on training data, and 10-fold cross validation for determining the optimum number of components. That optimum number, the one that minimized validation set errors, was 4 for each subject. The union of selected electrodes for all four components was then used to build a new PLS classifier using the training set data, as in the heuristic and frontal sets. For subject 212, that union was 19 (out of 21) electrodes across the four factors. For subject 220, 6 electrodes were in the union set. We summarized the selected electrodes and conditions of each model in Table 3. These served as the *oversampled* sets described in Table 1. We also produced two *critically* sampled sets, on which retained the first four electrodes indicated by their order of importance within the first two PLS factors. The second set retained three such electrodes. We observed that we could produce common sets for both subjects by including electrodes Cz and T5 for both subjects, although each of these electrodes was only indicated in one of each subject’s optimal set. Our thinking here was to produce a set that could be used across subjects, retaining the important electrodes from each subject. The two critically sampled sets were [Cz, T5, T6, Oz] or [T5, T6, Oz]. Thus, these electrodes sets met two criteria: they had the greatest sum of PLS weights in the first and second components, and they were indicated in this way for at least one subject.

Table 3. Statistically selected sets of electrodes for PLS classifier in two subjects.

Subject	Optimal/Maximum numbers of Components in PLS Classifier	Statistically Selected Electrode Set (not in order of importance)							Number of Electrodes
212	4 / 10	FP1	FPz	FP2	F7	F3	Fz	F4	19
		F8	T3	C3	Cz	C4	T4	P3	
		Pz	P4	T6	Oz	O2			
220	4 / 10	FP1	C4	T5	P4	T6	Oz		6

We constructed and tested the classifier as for the heuristic and frontal sets, then corrupted the data with noise and re-tested. The results were not surprising, in that SNR caused the accuracy to degrade smoothly and in roughly the same way as in the other frontal and heuristic simulations (Figure 5). In the figure, the two subjects' results are plotted for each of two levels of reduction. The first level is the "optimum" electrode set chosen by our algorithm so as to minimize classification error in cross-validation tests (S 212-19 electrodes, S 220-6 electrodes). The critical levels of reduction are S 212-3, S 212-4, S 220-3, S 220-4 for the two subjects and the three- and four-electrode sets respectively. For S 212, the optimal set of 19 electrodes was comparable to the full set of 21 electrodes, and the critical set of three electrodes produced results that were as good as or better than the 12- and 4-electrode sets chosen manually. For S 220, the optimal set of 6 electrodes yielded accuracies comparable to those of the 21-, 12-, and 4-electrode sets chosen manually. Some degradation of TPC occurred for with the four-electrode set for S212 but not for S22. Substantial degradation of TPC occurred for both subjects with the three-electrode set. In S 220, the critical set of 3 electrodes was clearly less successful than any of the manually selected sets. These results are only a coarse indication of what may be possible with automated selection. Nevertheless, as we found with the manual selection methods, automatically selected sets of 4 to 6 electrodes can support a classifier that performs well at SNRs above -6 dB.

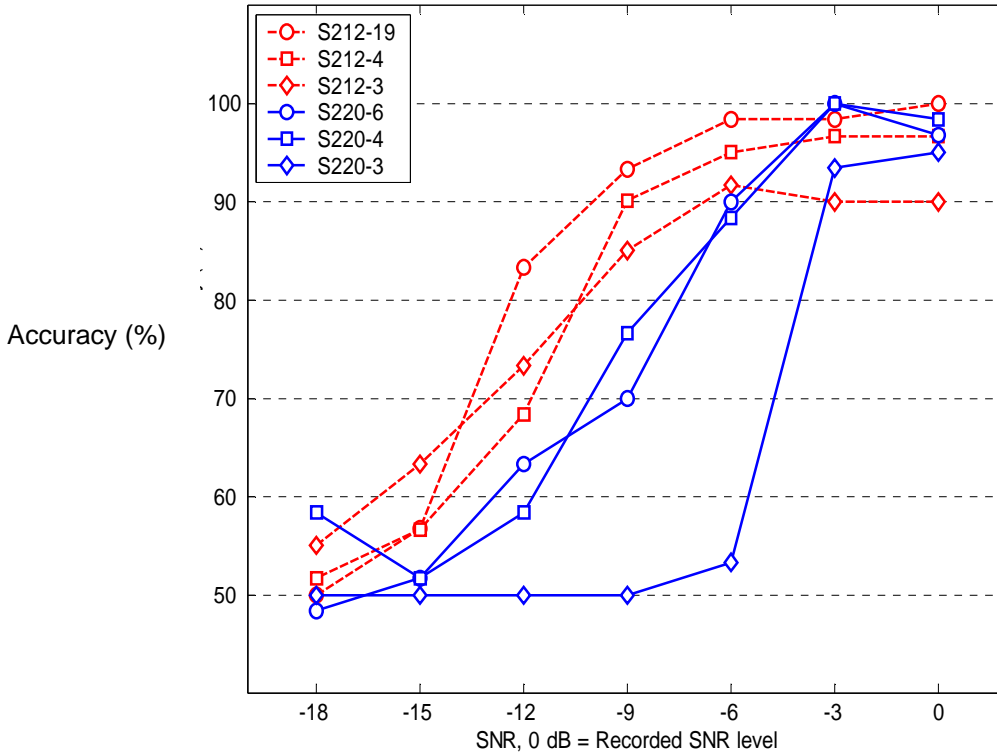


**Figure 5:** Classification accuracy for statistical electrode selection versus SNR in subjects 212 and 220. The three levels for each subject are the optimal set and the sets which contain the three or four most influential electrodes among both subjects.

### 3.4 Sample EEG Spectra

Spectra for a single EEG epoch of the four electrodes in the first critical set appear in Figures 6A and 6B. These figures show that the separation of single-trial spectra varies by electrode and subject. In S220 the spectral differences are clear and in the expected direction, but unclear for S212. Accordingly, some epochs are easily classified, while others lead to misclassification. Our KPLS classifier finds the set of components that maximally separates the two classes, leading to the highest TPCs for a given electrode set and subject.

## 4 Conclusions

Our methods and results successfully assessed the impact of electrode set size and reduced SNR on a real-time EEG-based fatigue classification algorithm. Overall, the results indicate that, our implementation of a PLS classifier functions robustly in the presence of noise. Even for arbitrarily selected sets of as few as four electrodes, with midline or frontal placement, TPCs ranging from 82% to 90% at an SNR of -6 dB. For larger arrays, TPCs ranged up to 99% at the -6 dB SNR level. This is a level at which the power of external noise is three times greater than the EEG signal itself. In laboratory or clinical settings, such a poor SNR would be considered unacceptable and nearly impossible to work with. We expect that operational settings will be noisier than the laboratory, but that SNRs of -6 dB or less should be easily avoided with proper precautions for shielding, grounding, and resistance to motion artifact. We note that the definitions of SNR differ for the simulated and test data. In particular the simulation SNR is known (ratio of AR process signal power to noise power), but for the real EEG data the signal is not known. We arbitrarily set the SNR of the EEG 0 dB and adjusted SNR according to the power of the added noise. In effect, this underestimates the true SNR of the EEG signal, which typically has positive SNR, and makes our results conservative with respect to real-world EEG recordings.

We conclude that robust, real-time classification of EEG patterns associated with fatigue is feasible in noise of up to -6 dB and with as few as four well-placed active electrodes. At present, the results indicate feasibility in a limited context (two subjects) and for unspecific fatigue conditions. Future work should consider extending these results to more subjects and experiment types. In particular, the dissociation of mental or cognitive fatigue from general fatigue and sleepiness must be properly controlled.

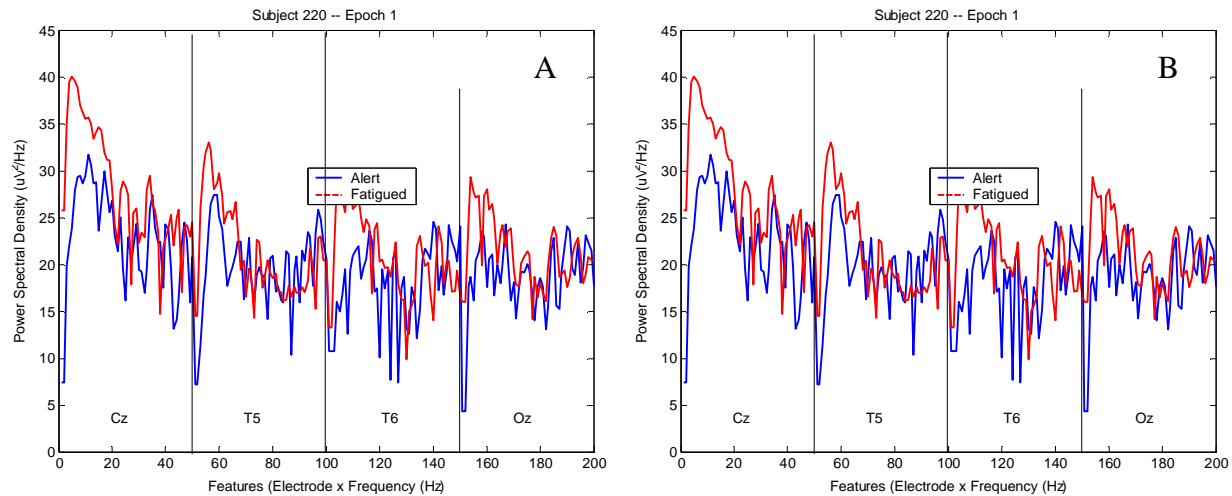


**Figure 6:** **A.** Spectra of a single EEG epoch for S212 in alert and fatigued conditions for electrodes in one statistically selected “critical” set. Frequency is numbered in feature space, as input for classification. Frequencies at each electrode range from 0-30 Hz. **B.** Corresponding spectra of a single EEG epoch for S220.

## 5 References

- Anderson, C.W., Stolz, E. A. and Shamsunder, S. (1995). Discriminating mental tasks using EEG represented by AR models. Proceedings of the 1995 IEEE Engineering in Medicine and Biology Annual Conference, September 20-23, Montreal, Canada.
- Bell, A. J. and Sejnowski, T. J. (1995). An information maximisation approach to blind separation and blind deconvolution, *Neural Computation*, **7**, 1129-1159.

- Caldwell, J., Caldwell, J. L., Brown, D., Smythe, N., Smith, J., Mylar, J., Mandichak, M. and Schroeder, C. (2003). The Effects of 37 Hours of Continuous Wakefulness on the Physiological Arousal, Cognitive Performance, Self-Reported Mood, and Simulator Flight Performance of F-117A Pilots. AFRL-HE-BR-TR-2003-0086. Brooks City Base, TX: U.S. Air Force Research Laboratory.
- Gevins, A. S., Bressler, S. L., Cutillo, B. A., Illes, J., Miller, J. C., Stern, J. and Jex, H. R. (1990). Effects of prolonged mental work on functional brain topography. *Electroenceph. clin. Neurophysiol.* **76**, 339-350.
- Hayes, M. H. (1999). *Statistical Digital Signal Processing and Modeling*. New York, Wiley.
- Makeig, S. and Inlow, M. (1993). Lapses in alertness: coherence of fluctuations in performance and the EEG spectrum. *Electroencephalogr. Clin. Neurophysiol.* **86**, 23-35.
- Rosipal, R., Trejo, L. J. (2001). Kernel partial least squares regression in reproducing kernel hilbert space. *Journal of Machine Learning Research*, **2**, 97-123.
- Rosipal, R., Trejo, L. J. and Matthews, B. (2003). Kernel PLS-SVC for Linear and Nonlinear Classification. In *Proceedings of the Twentieth International Conference on Machine Learning (ICML-2003)*, pp. 640-647, Washington, D. C.
- St. John, M., Kobus, D. A., & Morrison, J. G. (2003, December). DARPA Augmented Cognition Technical Integration Experiment (TIE). Technical Report 1905, SPAWAR Systems Center, San Diego.
- Trejo, L. J., Kochavi, R., Kubitz, K., Montgomery, L. D., Rosipal, R. and Matthews, B. (2004, October). Measures and Models for Estimating and Predicting Cognitive Fatigue. 44th Society for Psychophysiological Research Annual Meeting (SPR'04), Santa Fe, NM.
- Trejo, L. J., Wheeler, K. R., Jorgensen, C. C., Rosipal, R., Clanton, S. T., Matthews, B., Hibbs, A. D., Matthews R. and Krupka, M. (2003). Multimodal Neuroelectric Interface Development. *IEEE Transactions on Neural Systems and Rehabilitation Engineering*, **11**, 199-204.